



Computation of the Electric Field and Voltage Distributions over the Polluted Surface of Silicone-Rubber Insulators

Adnan S. Krzma and Mahmoud Y. Khamaira

Department of Electrical and Computer Engineering, Elmergib University, Al Khoms, Libya.

ARTICLE INFO

Article history:

Received: 13 January 2018;

Received in revised form:

24 February 2018;

Accepted: 5 March 2018;

Keywords

Silicone rubber outdoor Insulator, Electric field, Electrical potential, Finite Element Method (FEM), Pollution.

ABSTRACT

This paper investigates the performance of an 11 kV silicone rubber (SiR) outdoor insulator when subjected to an alternative voltage at 50 Hz. The electrical field and potential distributions over the insulator surface were computed and analysed using the Finite Element Method (FEM) COMSOL Multiphysics software. Comparative studies of field and equipotential contours for the insulator under dry clean and uniformly contaminated surface conditions are presented. The surface power dissipation along insulator surface is calculated. The critical of high field regions on SiR surfaces were identified and the power dissipated in the pollution layer along insulator profile was revealed. This study showed useful information about the surface heating which, might be help to predict any dry band formations along the leakage path of the insulator and to evaluate the insulator characteristics and its behavior.

© 2018 Elixir All rights reserved.

Introduction

Outdoor polymeric insulators are becoming an attractive option for use in HVAC and HVDC power system lines. They are gradually replacing the conventional insulators used in transmission and distribution systems. Compared with ceramic and glass insulators, silicone rubber insulators are light in weight, possess good electrical strength, easy to handle and transport and ultimately have reduced breakage. More importantly, polymeric materials such as SiR have hydrophobicity transfer materials, which ensures improved performance in contaminated environments [1, 2]. In the presence of the moisture, hydrophobicity prevents the formation of a water film, therefore minimising leakage current and the probability of dry band arcing.

Polymeric materials, however, suffer from tracking and erosion. They are susceptible to chemical changes when subjected to electrical, and environmental stresses during the service period. More importantly, the electric stress on the polymeric insulator under both normal operating and transient over-voltage conditions. The high field regions at the surface of the insulator especially near to the high voltage and the ground terminal can cause corona and discharges on the surface and this may eventually lead to complete flashover or degrade the insulator [3, 4]. Therefore, knowing the electric field along the insulator profile is very important and highly desired [5, 6].

In this paper, silicone rubber outdoor insulator used for 11 kV system voltage is modelled using a commercially available FEM, COMSOL Multiphysics software. The main objective of the simulation was to evaluate the electrical performance of the polymeric insulator. The voltage profiles along the insulator surface for dry-clean and wet-polluted insulators were computed. The equipotential lines of the SiR insulator model were also calculated.

For wet-polluted insulator, the tangential electric field along the leakage path of the insulator was calculated. The surface power dissipation on the pollution layer along insulator surface was calculated.

Insulator profile and computational modeling

The insulator investigated in this study is an insulator rated at 11 kV. The dimensions and geometry of the insulator are shown in Fig 1.

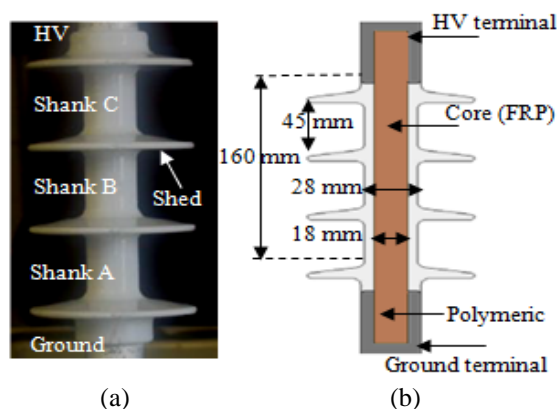


Figure1. An 11 kV silicone rubber insulator: (a) insulator geometry (b) cross-sectional profile and dimensions.

Silicone rubber insulator comprises of three main parts; insulator housing, metal end fitting and the fiberglass (FRP) core. The insulating housing is made of SiR material with a relative permittivity of $\epsilon_r = 2.9$. The metal fittings used for the high voltage energisation and ground terminals are made of the aluminium. These end fittings are attached to an 18 mm diameter fibre rod at a separation distance of 160 mm. The rod with a relative permittivity of $\epsilon_r = 7.1$ is crimped in the middle as a core to enhance the mechanical strength.

The insulator has 4-sheds with a diameter of 90 mm of each shed and spacing distance of 45 mm along the insulator

unit. The measured creepage distance along the insulator surface is about 375 mm. Both SiR material and fiberglass core in this simulation were assumed to be perfect insulator with conductivity of 1.0×10^{-13} S/m. The pollution layer over the insulator surface is assumed to be uniform with 0.5 mm thickness [7]. The conductivity of the pollution layer was adopted from the laboratory measurements with a value of 1.0×10^{-6} S/m. Detailed electrical properties used for insulator modelling are given in Table 1.

Table 1. Material properties for the used insulator.

Materials	Relative Permittivity,	Conductivity, σ (S/m)
Aluminium end fittings	1.0	26.31×10^6
Silicone Rubber	2.9	1.0×10^{-13}
FRP core	7.1	1.0×10^{-13}
Pollution layer	81	1.0×10^{-6}
Air background	1.0	1.0×10^{-13}

An AC voltage of 18 kV at 50 Hz is energised to the top high voltage terminal while the bottom terminal is connected to the ground (0 V). The energisation voltage corresponds to the peak value of the potential that applied to the insulator according to the IEC 60507 standard [8]. The air space surrounding the insulator is simulated adequately large to reduce its effect on the distribution of potential along the insulator profile and close to the electrodes. The outer edges of air region were assigned with a boundary of zero external current and electromagnetic sources, therefore representing a physical system that is an isolated open space.

Finite Element Method [FEM]

The silicone rubber insulator described in the previous section was drawing using AutoCAD software tools and saved in an extension file of dxf format. The insulator was then imported to the COMSOL Multiphysics software, and the boundary conditions were applied. In this model, as the insulator structure is cylindrical in shape, therefore, the modelling can be simplified into a two dimension (2D) symmetric model in preference to a full three dimension (3D) model that uses much of computer memory. This simplification saves the considerable size of memory and processing time without affecting the accuracy of the simulation results. In addition, using symmetric model, only half of the insulator structure was created, as shown in Figure 2.

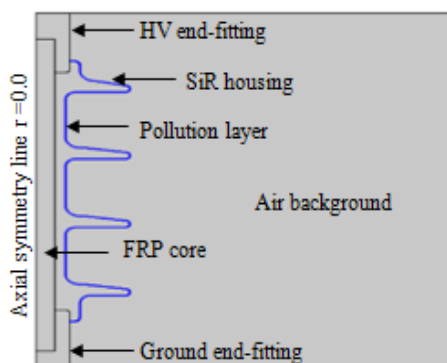


Figure 2. Two dimensions (2D) axis symmetric model for a polluted insulator.

After completing the stages of the model structure, specifying material properties and boundary conditions, the entire geometry regions except the end fitting parts were divided into small non-overlapping, non-separated triangular elements as illustrated in Figure 3. This process is called meshing process.

To improve and enhance the accuracy of the simulation results, the number of meshing element was increased in the region along the insulator surface where the electric field intensity is found to be higher.

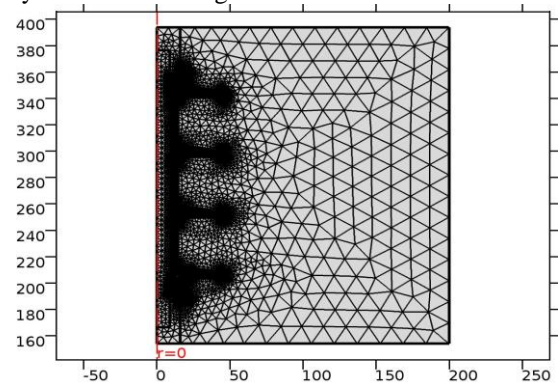


Figure 3. Mesh discretisation of insulator domain.

The insulator model was carried out in the FEM analysis using Quasi-Static Electric mode, which assumes that electromagnetic fields and currents varying slowly [9]. This assumption is valid for insulator problems and many other HV applications that operate at 50 Hz power frequency. The potential and electric field computations are calculated by solving the differential equation in the software given by equation (1).

$$-\nabla \cdot (\epsilon_0 \epsilon_r \nabla v) / \partial t - \nabla \cdot (\sigma \nabla v - J^e) = Q_j \quad (1)$$

Where J^e : External current density (A/m^2)

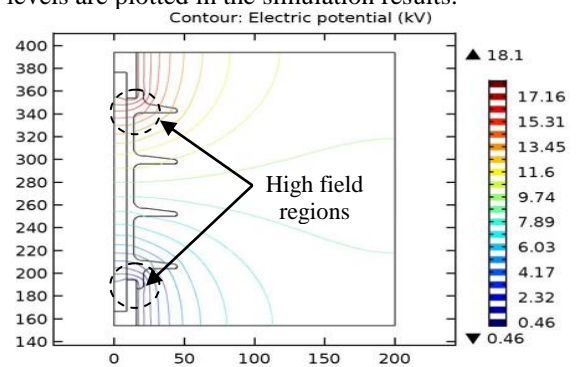
Q_j : Current source (A/m^3)

σ : Electric conductivity (S/m)

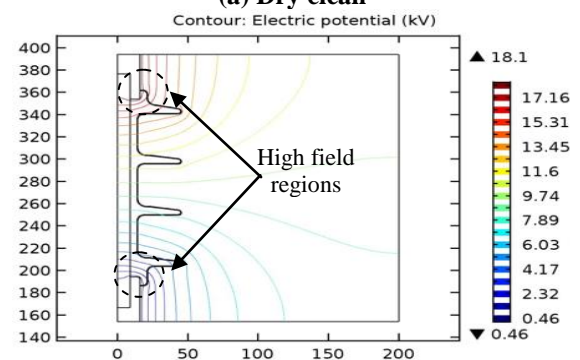
ϵ : Permittivity

Simulation results and discussion

The equipotential lines of the SiR insulator model under clean and wet polluted conditions are illustrated in Figure 4 (a) and Figure 4 (b) respectively. The lines are simulated at 5% voltage interval, so a total of 20 equipotential line levels are plotted in the simulation results.



(a) Dry clean



(b) Wet polluted

Figure 4. Equipotential lines along the surface profile of the dry clean and wet polluted SiR insulator.

As can be seen from both Figures, the contours are usually concentrated close to metal fitting electrodes. This indicating to the high electric field concentrated in these regions. Under wet polluted conditions, the equipotential lines are found to be more uniformly spread compared with those obtained from the dry clean surface. This behaviour occurs due to the presence of the resistive pollution layer which helps to redistribute the concentrated lines widespread along the surface profile.

The calculated voltage distributions along the leakage profile of the insulator under both surface conditions are shown in Figure 5. The creepage distance is measured along the SiR surface, starting from the ground and ending at the high voltage terminal (375 mm). An increment trend is observed for both curves when shifting toward the energisation end. The voltage profile along dry clean surface shows a high potential gradient at both ends, demonstrating high field regions on the insulator surface. This can be correlated with the equipotential lines obtained in Figure 4 (a) where the line concentration is close to the insulator terminals. For the wet polluted surface, the voltage profile seems to be more uniform and smoother than the profile for the clean insulator. This attributed to the equally spread distribution of the equipotential lines shown in Figure 4 (b).

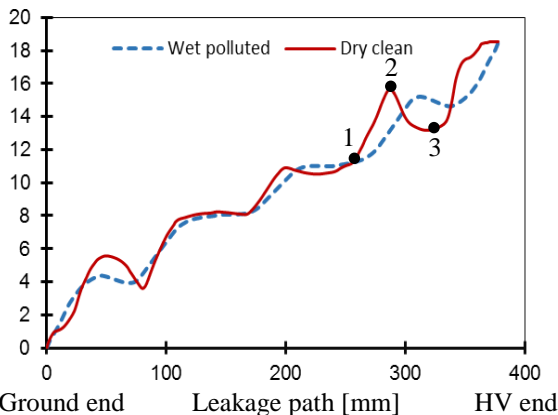


Figure 5. Voltage profile along the SiR insulator surface.

The dry clean surface also shows curve undulations mainly at the region close to the insulator terminal ends. These undulations are caused by the equipotential lines that cross the insulator surface at more than one point (1, 2, and 3) as illustrated in Figure 6.

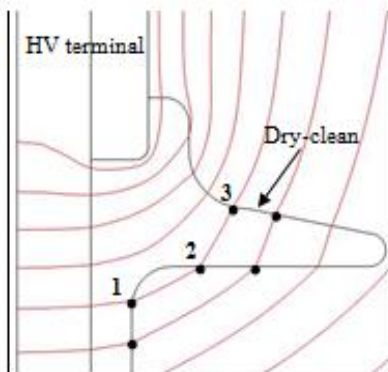


Figure 6. Zoomed in the equipotential line contours of the dry clean surface close to the HV terminal end.

The same voltage level appears at different locations along the leakage distance causing a non-smooth voltage profile. The undulations are not observed on the potential profile under the polluted condition. This can be explained by

the equipotential line only crosses the surface at one single point, as seen in Figure 7.

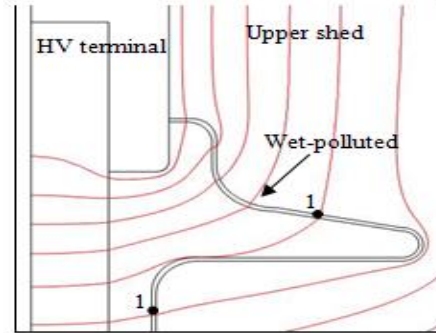


Figure 7. Zoomed in the equipotential line contours of the wet polluted surface close to the HV terminal end.

Electric field distribution along the wet polluted insulator

Figure 8 shows the plot results of electric field distribution along the leakage distance of the insulator under wet polluted surface condition. The simulated electric field was computed representing the tangential electric field along the insulator surface. The graph, in general, demonstrates a similar trend of electric field distribution between the ground and HV ends. The highest tangential field obtained on the surface is that near to the metal fitting electrodes with magnitude value of 1.9 kV/cm. Peaks of tangential field can be also seen in the shank regions where is the field magnitude reaching about 1 kV/cm. These peaks show a good correlation with the equipotential results and voltage profile concerning in the previous section.

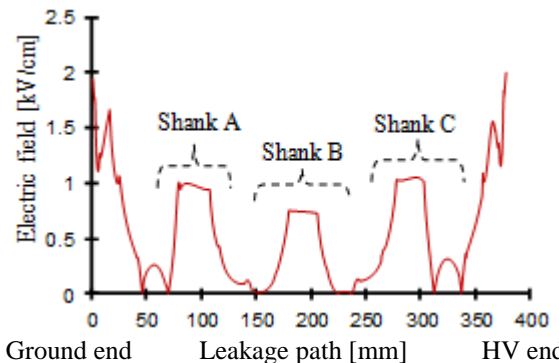


Figure 8. Tangential electric field along the leakage path for insulator under wet polluted surface condition.

From the equipotential lines illustrated in Figure 4(b), it is recognised that the electric field in the shanks areas tends to pass tangentially to the insulator surface, therefore enhancing to increase the electric field at the surface regions between 69 mm and 120 mm (shank A), 159 mm and 220 mm (shank B) and 240 mm and 312 mm (shank C) along the leakage distance and this can be clearly seen in Figure 9.

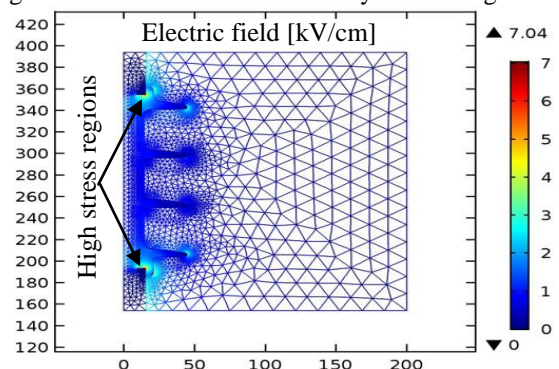


Figure 9. Electric field concentrations along the surface profile of a polluted insulator.

The electric field in the regions of the upper shed surface near to the ground electrode (between 44 mm and 69 mm) and the bottom shed surface at high voltage end (between 312 mm and 335 mm) are significantly low. This is because the tangential field component is run in the opposite direction of the leakage current along the SiR surface.

Power dissipation in the pollution layer along insulator surface

Discharge activities and dry band formation on the surface of the SiR insulator are relatively correlated with the high electric field. With the presence of the wet pollution layer on the surface, the flow of the leakage current is mainly driven by the electric field, in particular, the tangential component. This current will cause power dissipation leading to resistive heating in the pollution layer which, consequently, will dry out the water and thus leading to the formation of dry bands on the insulator surface. The surface power dissipation in the pollution layer per unit surface area along the leakage path was calculated in [10]:

$$P_{\Omega} = \sigma \cdot E_t^2 \cdot t_p \quad (2)$$

Where E_t : the tangential electric field (V/m)

t_p : the thickness of the pollution layer along the leakage path (mm)

σ : the conductivity of the pollution layer along the leakage path (S/m)

The surface power dissipation in the pollution layer along the leakage path is shown in Figure 10 and computed using the equation 2 and the tangential electric field results obtained from the Figure 9. The thickness and the conductivity of the pollution layer used are the same values given and detailed in Table 1.

The calculation of power dissipation was carried out through programming the equation in the COMSOL software. Figure 10 shows two power peaks close to the end terminals in the same regions where the highest tangential electric field observed. The highest dissipated power value observed is about 18 W/m^2 . Peaks of the dissipated power can be also seen the shanks regions along the insulator surface as expected with magnitude value of 5 W/m^2 .

It can be predicted that electric discharges and the formation of dry bands are probably to occur near the end terminals and shanks regions where the highly tangential field and long heating effects. Continuous heating on the SiR surface could destroy its hydrophobicity and, therefore, leads to degradation of the insulator on the long term.

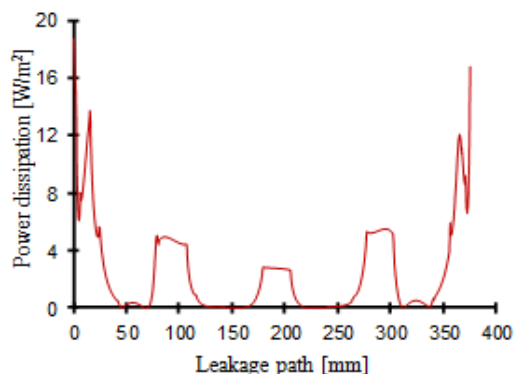


Figure 10. Surface power dissipation in pollution layer along polluted insulator surface.

Conclusion

The electrical performance of silicone rubber outdoor insulator was investigated in this paper. The potential and electric field distributions along the surface profile of silicone rubber insulator have been studied using the COMSOL

Multiphysics Finite Element Software. An ideal model has been adopted for an easily simulation the laboratory test conditions. The simulation results under dry clean and wet polluted surface conditions reveal the highly electric field region on the insulator surface as expected. In particular, near the end terminals and shanks regions. This favourable finding gives a good correlation between the two methods of simulation analysis and laboratory work. The power dissipation on the surface of the wet polluted insulator is relatively proportional to the electric field strength, particularly, the tangential field. This field has an effect on the developments of the surface leakage current leads to resistive heating in the pollution layer, thereby, the formation of dry bands. These simulation results provide useful information about surface heating that might be used to predict the formation of the dry band along the leakage path of the insulator.

References

- [1]A. I. Elombo, J. P. Holtzhausen, H. J. Vermeulen, P. J. Pieterse, and W. Vosloo, "Comparative evaluation of the leakage current and aging performance of htv sr insulators of different creepage lengths when energized by AC, DC+ or DC-in a severe marine environment", *IEEE Transactions on Dielectric and Electrical Insulation*, vol.20, no.2, pp.421–428, 2013.
- [2]G. Bruce, S. Rowland, and A. Krivda, "Performance of silicone rubber in DC inclined plane tracking tests", *IEEE Transactions on Dielectric and Electrical Insulation*, vol.17, no.2, pp.521–532, 2010.
- [3]A. S. Krzma, M. Albano, and A. Haddad, "Flashover influence of fog rate on the characteristics of polluted silicone rubber insulators," in 2017 52th International Universities Power Engineering Conference (UPEC), Crete, Greece, pp. 1–6, 2017.
- [4]A. S. Krzma, M. Albano, and A. Haddad, "Comparative performance of 11kV silicone rubber insulators using artificial pollution tests," in 2015 50th International Universities Power Engineering Conference (UPEC), Stoke On Trent, United Kingdom, pp. 1–6, 2015.
- [5]Z. Farhadinejad, M. Ehsani, I. Ahmadi- Joneidi, A. A. Shayegani, H. Mohseni, "An investigation of the effect of UVC radiation on thermal, electrical properties and morphological behavior of silicone rubber insulators" *IEEE Transactions on Dielectrics and Electrical Insulation*, Vol. 19, No. 5, Page(s): 1740- 1749, October 2012.
- [6]M. H. Nazemi and V. Hinrichsen, "Experimental Investigations on Water Droplet Oscillation and Partial Discharge Inception Voltage on Polymeric Insulating Surfaces under the Influence of AC Electric Field Stress," *IEEE Transactions on Dielectrics and Electrical Insulation*, vol.20, no. 2, pp.443-453, 2013.
- [7]R. Abd-Rahman, A. Haddad, N. Harid, and H. Griffiths, "Stress control on polymeric outdoor insulators using Zinc oxide microvaristor composites," *IEEE Trans. Dielectr. Electr. Insul.*, vol. 19, no. 2, pp. 705–713, Apr. 2012.
- [8]IEC 60507:2013, 'Artificial pollution tests on high-voltage ceramic and glass insulators to be used on a.c. systems', 3rd edition.
- [9]COMSOL Multiphysics User's Manual," ed: Version 5.2.
- [10]A.S.Krzma, "Comparative laboratory performance characterisation of silicone rubber textured insulators," PhD thesis, Advanced High Voltage Engineering Research Centre, Cardiff University, 2016.